Rapid, Controllable Fabrication of Regular Complex Microarchitectures by Capillary Assembly of Micropillars and Their Application in Selectively Trapping/Releasing Microparticles

Dong Wu, Si-Zhu Wu, Shuai Zhao, Jia Yao, Jiang-Nan Wang, Qi-Dai Chen, and Hong-Bo Sun**

***A** simple strategy to realize new controllable 3D microstructures and a novel method to reversibly trapping and releasing microparticles are reported. This technique controls the height, shape, width, and arrangement of pillar arrays and realizes a series of special microstructures from 2-pillar-cell to 12 cell arrays, S-shape, chain-shape and triangle 3-cell arrays by a combined top down/bottom up method: laser interference lithography and capillary force-induced assembly. Due to the inherent features of this method, the whole time is less than 3 min and the fabricated area determined by the size of the laser beam can reach as much as 1 cm^2, which shows this method is very simple, rapid, and high-throughput. It is further demonstrated that the 'mechanical hand'-like 4-cell arrays could be used to selectively trap/release microparticles with different sizes, e.g., 1.5, 2, or 3.5 μm, which are controlled by the period of the microstructures from 2.5 to 4 μm, and 6 μm. Finally, the 'mechanical hand'-like 4-cell arrays are integrated into 100 μm-width microfluidic channels prepared by ultraviolet photolithography, which shows that this technique is compatible with conventional microfabrication methods for on-chip applications.*

1. Introduction

The ability to selectively trap and release micro-objects is highly demanded in the fields of cell culture and biomedical devices.[1] Optical tweezers[2] generated by the gradient force of a single strongly focused laser beam have been successfully used to manipulate microparticles from several micrometres to tens of nanometers. However, they require high laser intensities, which are usually harmful to biological cells and chemical reactions. To trap micro/nanoparticles, a variety of microstructures[3,4] have been prepared. For example, Leong et al.[3] first realized single-use, chemically triggered, reversible mobile grippers which can be used to manipulate micro-objects under the actuation of acetic acid and hydrogen peroxide. The gripper was remotely controlled by a magnet to move toward a bead and trap it. Pokroy et al.[4] reported a novel method to rapidly and simultaneously trap lots of particles by fabricating hierarchical helical structures. But these methods are usually complicated. In addition, in practical applications, the manipulation of micro-objects should have excellent selectivity. Here, we report the precise trapping and releasing of microparticles with specific sizes by large-area controllable microstructures, like 'mechanical hands', which

Dr. D. Wu, S.-Z. Wu, S. Zhao, J. Yao, J.-N. Wang, Prof. Q.-D. Chen, Prof. H.-B. Sun
State Key Laboratory on Integrated Optoelectronics
College of Electronic Science and Engineering
Jilin University
2699 Qianjin Street, Changchun, 130012, PR China
E-mail: chenqd@jlu.edu.cn; hbsun@jlu.edu.cn
Prof. H. B. Sun
College of Physics
Jilin University
119 Jiefang Road, Changchun, 130023, PR China

DOI: 10.1002/smll.201201689

NANO MICRO small

are rapidly realized by a kind of combined top-down/bottom-up method. The size of the particles being trapped can be controlled by adjusting the period of microstructures. This manipulation method features scalability, size-selectivity, and reversibility.

Recently, the combination of top-down/bottom-up technology[5] to realize controllable micro/nanostructures for broad applications has become a hot topic since it can realize a lot of functional microarchitectures which are difficult to obtain by a single technique. Top-down technologies[6] such as ultraviolet photolithography, electron beam lithography, focused-ion-beam, and laser direct writing have been widely used to fabricate well-controlled structures, but the achievable geometry is confined to a relatively simple morphology. In contrast, the bottom-up approach can assemble various complex microstructures from small solid components or molecules by weak forces, such as van der Waals forces, capillary forces, and chemical bonding forces, however, the regularity and controllability is a little poor.[7] By combining both methods, a variety of regular complex 3D microarchitectures—for example, ZnO flower arrays,[8] colloidal sphere spiral chains,[9] or carbon nanotube microwells[10]—have been realized. Among these methods, capillary force self-assembly of polymer micro/nanopillars has attracted great attention due to its many advantages, e.g., low cost, simplicity, and scalability. There are many works on the combination of capillary force self-assembly and top-down techniques. For example, Pokroy et al.[4] reported hierarchical helical arrays by capillary force assembly of micropillar arrays, which was fabricated by the two-step soft transfer of a silicon template prepared by UV lithography and plasma etching. Duan et al.[11] realized a series of complex nanopatterns at a 10 nm scale based on capillary force-induced cohesion of high-aspect-ratio nanostructures made by electron-beam lithography. Kang et al.[12] further controlled the shape and size of nanopillar assembly by adhesion-mediated elasto-capillary interactions and investigated their stability by surface chemistry. Although a variety of complex nanopatterns have been made, it is still attractive to assemble novel controllable microstructures. Moreover, many of these methods rely on expensive apparatus or complex multistep processes. Therefore, it is important to develop a simple, rapid, and high-throughput method for scalable fabrication of various complex micro/nanostructures at a level required for industrial applications.

Multibeam laser interference lithography[13] is a powerful technique to rapidly realize various functional micro/nanostructures with wafer-scales by the interference of multiple beams of light into the materials. In this paper, we report a new strategy to realize a series of capillary force-induced novel 3D microstructures with large-area by controlling the height, shape, width and arrangement of the pillar arrays which are realized by laser interference lithography wthin 3 min. We further demonstrate that the 'mechanical hand'-like 4-cell arrays can be used to effectively trap/release microparticles with different sizes, e.g., 1.5, 2, and 3.5 μm, whose sizes were determined by the period of the microstructures from 2.5 to 4 μm and 6 μm. The underlying physical mechanism of reversible particle micromanipulation is systemically investigated, and is attributed to the capillary force and the van der Waals force during the evaporation and immersion processes.

2. Results and Discussion

2.1. Regular Controllable Microstructures Realized by Pillar Arrays with Different Heights

Shown in **Figures 1**b–h are scanning electron microscopy (SEM) images of 2-pillar-cell, 4-pillar-cell, 6-pillar-cell, 9-pillar-cell, and 12-pillar-cell arrays fabricated by capillary force assembly of pillars with different heights. Firstly, 4 mm-period micropillar arrays with large areas were prepared by multibeam laser interference lithography. Then, the polymeric pillars were assembled into various complex patterns in liquid solvents under evaporation-induced capillary forces. According to our previous study,[14] the relative magnitude of the capillary force F_{att} and the supporting force F_s determine whether a needle is to stand upright or bend aside. The capillary force F_{att} is caused by the liquid surface tension during the solvent evaporation process:

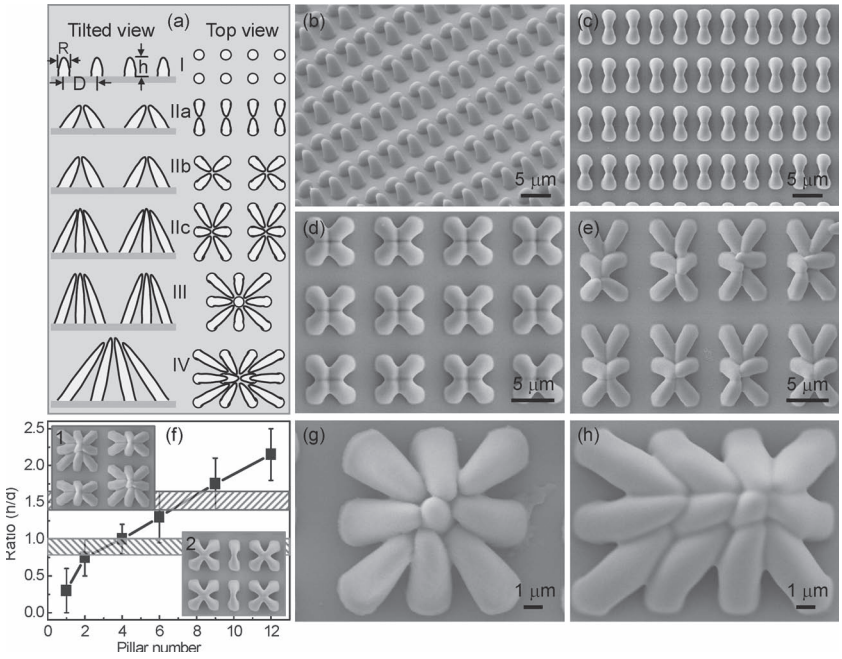

Figure 1. Regular controllable microstructures realized by capillary force assembly of pillar arrays with different heights. (a) Schematic diagrams for various assembled patterns by controlling the height of the pillars. (b,c) Tilted-view and top view SEM images of regular 2-cell arrays. (d,e,g,h) 4-cell, 6-cell, 9-cell, and 12-cell arrays, respectively. (f) The dependence relationship between the pillar number and the ratio (h/d).

$$F_{att} \sim 2\pi Rh\gamma \cos(\alpha/\delta) \quad (1)$$

The supporting force $F_s \sim ER^4d/h^3$ is defined as the critical force that causes the pillar bending, where h, R, d, and E are the height, width, period of pillar, and the Young's modulus, respectively. γ, α, and δ are the the surface tension, contact angle, and the space between the two pillars, respectively. The ratio (K) of F_{att} and F_s will determine the bending properties of the pillar arrays.

$$K = F_{att}/F_s \sim (2\pi\gamma/Ed) \cos(\alpha/\delta)h^4/R^3 \quad (2)$$

From this formula, we know that the height (h) and the width (R) of the pillars have a dramatic impact on the ratio *K*. If *K* is bigger than 1 ($F_{att} > F_s$), the pillars will bend together, or else, the pillars will keep straight. Therefore, we could control the balance of both forces and obtain different morphologies by designing the parameters of the pillars. In this work, we mainly focused on the height (h) and the width (R) of the pillars which was easily controlled by the spin-coating speed and the laser power. Firstly, the height of pillars was investigated in detail. The height from 1 μm to 9 μm was obtained by controlling the spin-coating speed from 200 to 3000 rpm/s. Because the value *K* is biquadratic to *h*, the pillars will significantly deform as the height increases, as shown in the schematic image of Figure 1(a). To verify our opinions, pillar arrays with different heights were obtained by controlling the thickness of the resin. Experimentally, we found that the pillar stood straight and didn't bend when the height was low (<2.4 μm) because the F_s was bigger than F_{att} ($K < 1$). As the height increased to 3 μm, the *K* became big so that the pillars began to bend and 2-pillar-cell arrays were obtained [Figure 1(b,c)]. We further investigated the physical process by in-situ optical microscopy, which revealed that 4-pillar-cell arrays were formed initially during the evaporation process [Figure S1(a–c)]. However, they were subsequently changed into 2-pillar cell arrays when the system dried [Figure S1(d)]. This suggests that in air the surface adhesion caused by short-range van der Waals force is not strong enough to overcome the pillar elasticity force of 4-pillar cell. So, the 2-pillar-cell arrays were obtained, which exhibited less tilted degree and smaller elastic force than those of 4-pillar-cell arrays. Generally, for this critical state, the value *K* could be considered as 1. After further increasing the pillar height to 4 μm, 4-pillar cell arrays [Figure 1(d)] were assembled because *K* increased to 3.16. Similarly, as the height increased to 5.3 μm, 6.9 μm, 8.6 μm, six cells [Figure 1(e)] and higher-order assembles [Figure 1(g,h)] were obtained, just as expected. Along the dependence relationship between the pillar number and the ratio (h/d) [Figure 1(f)], we can precisely design various regular micropatterns. Moreover, two kinds of microstructures, such as 2-cell and 4-cell [the inset 1 of Figure 1(f)], 6-cell and 9-cell [the inset 2 of Figure 1(f)] were simultaneously obtained for certain crossed height [the shadow region of Figure 1(f)]. The random nucleation and propagation could be alleviated by the sample-tilted evaporation method.[14](a)] Typically, the uniform assembled area could reach as much as 4×10^4 μm. If the interference laser beam possesses high uniformity, a patterned area with a wafer scale will be realized.[13c]

2.2. Anisotropic Regular 'S' and 'Chain-like' Array Microstructures Prepared by Controlling the Width of the Pillars

The above pillars are round and the supporting forces of the pillars along all directions are constant. Here, to obtain novel anisotropic microstructures, the round shape was changed into the elliptical one. The F_{att} is linear dependence to the width of the pillar while the F_s is biquadratic to the R. So, the relative magnitude of the F_{att} and F_s could be controlled by changing the shape of the pillar [**Figure 2**(b)]. Shown in Figure 2(a) are

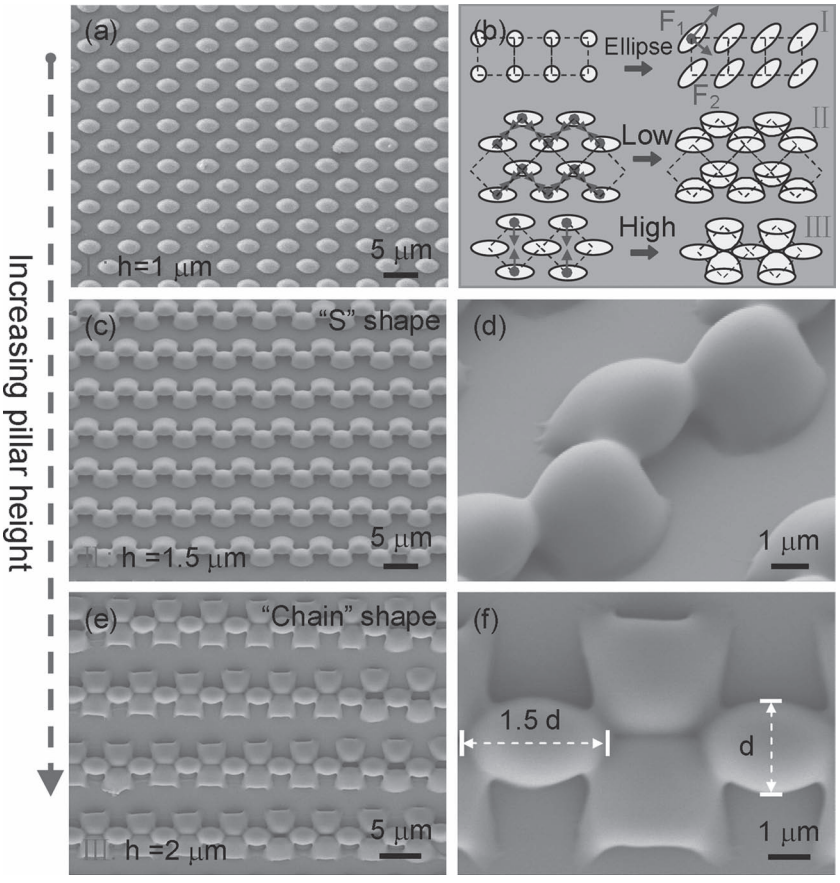

Figure 2. Anisotropic regular "S" and "Chain-like" microstructures prepared by controlling the width of the pillars. (a) The 1 μm-height elliptical pillars which were realized by modified laser interference lithography. (b) Schematic diagrams for various assembled patterns by controlling the shape and the height of the pillars. (c,d) Top-view and magnified SEM images of the "S" shape arrays assembled by 1.9 μm-height pillars. (e,f) Top-view and magnified SEM images of the chain-like arrays assembled by 2.6 μm-height pillars.

small NANO MICRO

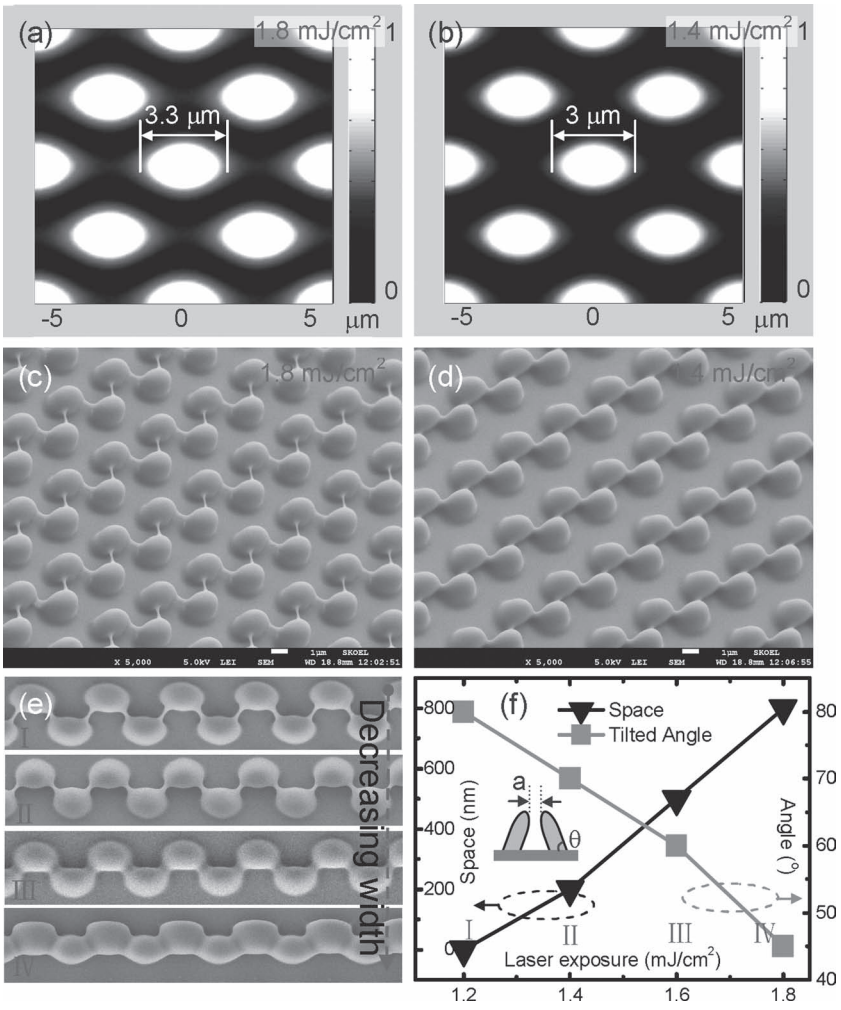

Figure 3. A series of complex microstructures realized by controlling the width of elliptical pillars. (a,b) Simulated laser intensity distributions with different exposures, 1.8 mJ/cm^2 and 1.4 mJ/cm^2, respectively. It was obvious that the pillars became wide as the laser exposure increased. (c,d) SEM images of the corresponding "S" shape microstructures. (e) A series of "S" shape microstructures by decreasing laser exposure. (f) The dependence relationship among the laser exposure, the space, and the tilted angle.

the elliptical pillars prepared by modified laser interference lithography.[15] Along the long-axis direction of the elliptical pillar, the supporting force (F_1) is much bigger than the one (F_2) along the short-axis direction. So, the pillars don't bend along the long-axis direction. Shown in Figure 2(c,e) are two kinds of assembled microstructures, "S" shape and chain shape, prepared by controlling the height of the elliptical pillars. When the height is lower than 1 μm, the supporting forces along both directions are so big that the pillars stand straight [Figure 2(a)]. As the height increases to 1.9 μm, the supporting force significantly decreases. The pillars bend along the short-axis direction and form regular "S" shape arrays with large area [Supporting Information Figure S2] during the solvent evaporation process. From the magnified SEM image, we could see that the adjacent pillars connected with each other and formed the stable state. However, when the height of the pillar was increased to 2.6 μm, the opposite pillars attracted each other because of the increased capillary force and the decreased supporting force. In this case, a kind of new microstructure—chain-like arrays [Figures 2(e,f)]—was obtained. Therefore, by designing the shape and the height of the pillars, a series of novel controllable microstructures were prepared.

Besides the height and the shape of the pillar, we could control the width of pillar for various microstructures by changing the laser intensity. Shown in **Figure 3**(a.b) are the simulated laser intensity distribution with different exposure 1.8 mJ/cm^2 and 1.4 mJ/cm^2. It was obvious that the pillars became wide as the laser exposure increased. This will have an important impact on the force balance of the pillars. Shown in Figure 3(c,d) are the fabricated "S" shape microstructures under 1.8 mJ/cm^2 and 1.4 mJ/cm^2 laser exposure. As the width of the pillar increased, the supporting force became big and the tilted angle decreased. It is also interesting to find that adjacent pillars were connected by 150 nm-diameter nanowires, which are dependent on the development conditions.[16] To systemically investigate the relationship between the microstructures and the laser exposure, laser exposure from 1.2 to 1.8 mJ/cm^2 was adopted. We can obtain "S" shape arrays with different tilted angles, as shown in Figure 3(e). Too small exposures (<1 mJ/cm^2) will not induce sufficient polymerization of the resin while too big exposure (>2 mJ/cm^2) will caused that the pillar would not bend. Shown in Figure 3(f) are the dependence between the tilted angle and the laser exposure. As the laser exposure increased, the angle became big because of the enhanced width of the pillars. The width increased from 3 μm to 3.5 μm when the laser exposure was changed from 1.2 to 1.8 mJ/cm^2.

2.3. 3-Pillar-Cell Arrays and Network Microstructures Prepared by Designing the Arrangement of the Pillar Arrays

The above microstructures were assembled based on square pillar arrays realized by four beams laser interference lithography. To assemble novel microstructures, triangle-arrangement pillar arrays were prepared by three beams interference lithography [Supporting Information Figure S3], as shown in **Figure 4**(a). Figure 4(b) shows top-view SEM image of regular triangle pillar arrays prepared by the resin NOA 61. When the height is less than 3 μm controlled by the resin thickness, the pillars stand straight because of the strong supporting force. After we increased the pillar height to 4 μm, three adjacent pillars were attracted together by capillary force during the solvent evaporation process. So, regular 3-pillar-cell arrays were self-assembled under optimal laser exposure (1.6 mJ/cm^2), as shown in the Figure 4(c). Too strong exposure

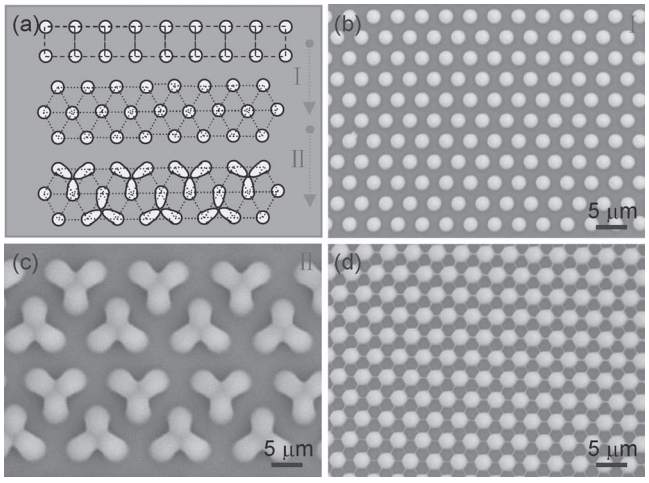

Figure 4. 3-pillar-cell arrays and network microstructures obtained by designing the arrangement of the pillar arrays. (a) Adjusting the arrangement of the pillars by three-beam laser interference lithography (I) and assembling triangle cell arrays by capillary force (II). (b) Triangle pillar arrays with height less than 3 μm. (c) 3-pillar cell arrays fabricated by capillary force assembly of the 4 μm height pillars. (d) Large area regular networks controlled by the developing conditions under strong laser exposure.

(>2 mJ/cm^2) also leads that the diameter of the pillar is too big to be assembled into 3-pillar cell arrays, as shown in Figure 4(d). In this case, it is also interesting to find that special kinds of networks, pillars and nanowires, formed, which is controlled by the developing conditions.

2.4. The Application and Physical Mechanism of Selective Particle Trapping and Releasing by the Assembled Microstructures

The ability to manipulate nanoparticle and microcells is highly desirable in biological and chemical researches. Here, we demonstrated that the capillary force-assembled 4-pillar cell arrays could be used as a mechanical hand for trapping nanoparticles, as shown in **Figure 5**(a). When the 2 μm-diameter particles were put into the pillar arrays in solvent, they were trapped by adjacent pillars due to the capillary force. In our experiment, we also found that the pillars preferentially bent towards the particles because a new capillary force between the pillars and particle appears [Figure S4(a)]. To verify our opinions, we prepared pillars with smaller-height (1.8 μm) which will not bend [Supporting Information Figure S4]. However, after adding particles, we found that these pillars bent towards the particles [Figures S4(b) and 4(c)] due to the new capillary force between the pillars and particles. In this situation, there are two kinds of the capillary forces: the pillar-to-pillar one and pillar-to-particle one, as shown in Figure S4(a). Moreover, because the space between the pillar and particle is much smaller than the one between adjacent pillars, the pillar-to-particle capillary force is much bigger than the pillar-to-pillar one, according to the formula (1). This is also the reason why the particles were easily trapped

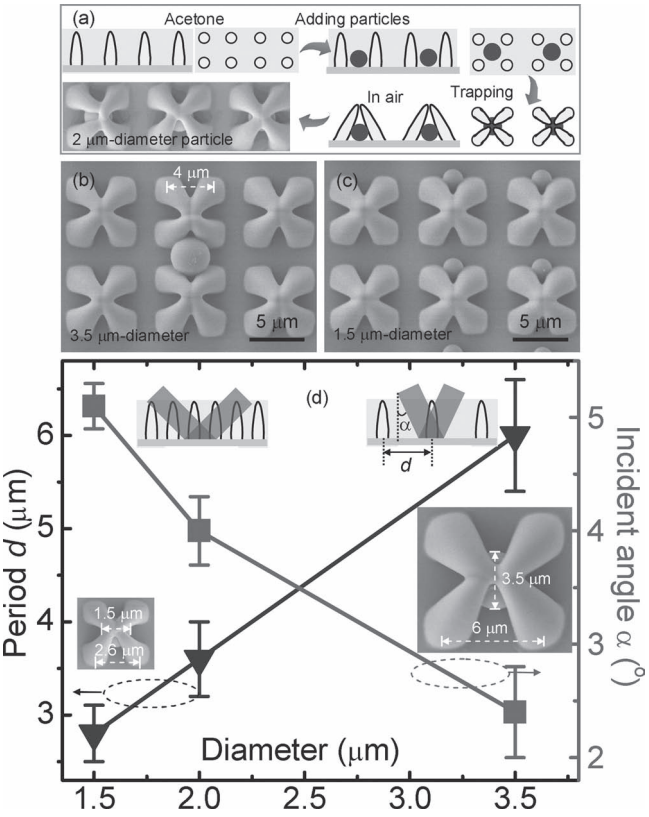

Figure 5. The selectively microparticles trapping by the assembled microstructures. (a) Schematic image of the trapping process. 2 μm-diameter microparticles were trapped by the assembled patterns which could be considered as a mechanical hand. (b,c) Too big (>3.5 μm) or too small particles (<1.5 μm) could not be effectively trapped, which demonstrated that the mechanical hand could have the ability to selectively trap microparticles. (d) Trapping different-size particles by designing suitable-period pillar arrays which could be precisely controlled by the interference angle.

by the pillar arrays. Moreover, we demonstrated that the mechanical hand-like arrays could selectively trap particles with special diameter, which was determined the period of the pillars. Too big (>3.5 μm) or too small particles (<1.5 μm) could not be effectively trapped, as shown in Figure 5(b,c). Here, owing to the excellent designability of laser interference lithography, the period of the pillars could be adjusted by changing the interference angles. To trap various particles, e.g. 1.5 μm or 3.5 μm, we prepared pillar arrays with different periods 2.6 μm and 6 μm under the interference angles 5.1° and 2.4°, as shown in Figure 5(d). Generally, the diameter of the trapped particles is linear dependence to the period of the pillars. According to this experimental result, we can get the relationship by theoretical fitting.

$$d = 1.8 \times d_p \tag{3}$$

Where d and d_p are the period of the pillars and the diameter of the trapped particles. Besides the particle diameter, the trapping efficiency also has been investigated. The trapping efficiency, defined as the ratio of the trapped particles to the total particles, is about 30 ± 10% with low concentration (10^{-4} g/mL). Too high concentration (>10^{-3} g/mL) will lead to

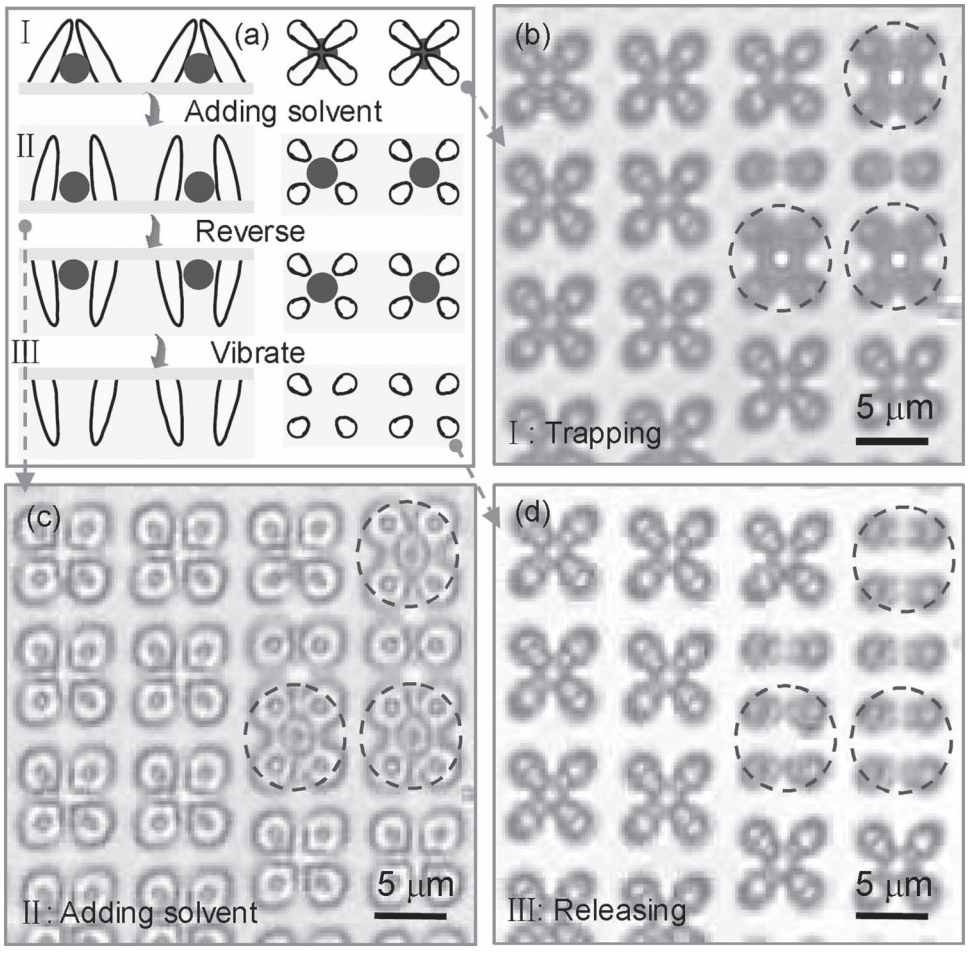

Figure 6. The reversible trapping and releasing process of the micromechanical hand. (a) Schematic diagrams for the experimental process: particles trapping, adding solvent, reversing the sample and vibrating it. (b–d) The particles being trapped/released by the assembled microstructures.

the disturbance between adjacent particles, as shown in Supporting Information Figure S5. Compared with the state-of-the-art methods,[3,4,17] this technology exhibited simultaneously rapidness and large-area. The whole time from microstructures fabrication to particles trapping is less than 10 min.

Besides the microobject trapping, the releasing function is also highly desirable in practical applications. Experimentally, when the micromechanical hand-like arrays [image I in **Figure 6**(a)] were put into the solvent, the pillar arrays basically recovered to upstraight position [image II in Figure 6(a)]. This is because the pillar/solvent van der Waals force happens in the presence of organic solvent, as shown in **Figure 7**. Firstly, the adjacent pillars bent together by the solvent evaporation-induce capillary force [Figure 7(a)]. Then, the pillar/pillar van der Waals force keeps the stable state in air after drying [Figure 7(b)]. When the assembled microstructures are immersed into solvent [Figure 7(c)], a new van der Waals force between the pillar and solvent happens. The F_{v2} will counteract the F_{v1} so that the pillar recovers the straight state [Figure 7(d)]. In addition, the swelling force may also enable the pillar to recover. As we know, the solidified polymer pillar is a kind of crosslinked

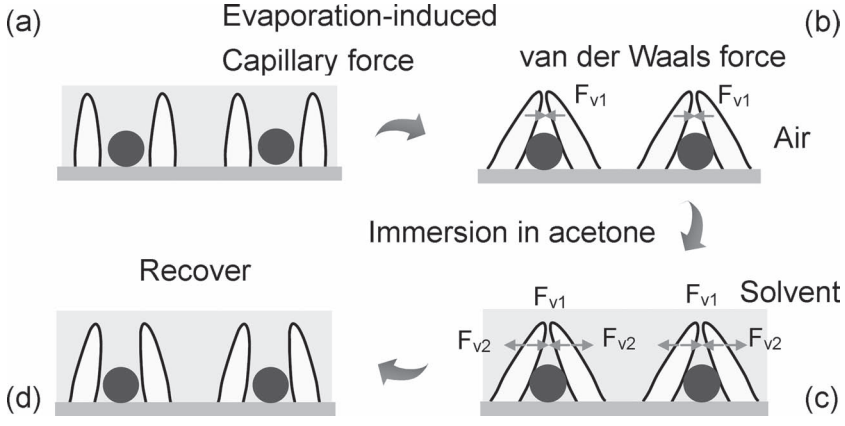

Figure 7. The physical mechanism of particles being trapped/released. (a) The particles were trapped by adjacent pillars under the solvent evaporation-induce capillary force. (b) The pillar/pillar van der Waals force (F_{v1}) keeps the stable state after drying. (c) A new van der Waals force between the pillar and solvent (F_{v2}) happens after solvent immersion. The F_{v2} will counteract the F_{v1} so that the pillar recovers straight state. (d) The pillar recovered straight and the particles were released by vibration.

photopolymer network[18], which will shrink and swell in the absence/presence of solvent. After the pillar arrays were reversed, the trapped micro-objects could be released after slight vibrate [The III image of Figure 6(a)]. Shown in Figure 6(b–d) are the experimental trapping and releasing process of micro-objects. Firstly, there are three microparticles trapped by three pairs of pillar arrays [Figure 6(b)]. After adding the solvent, the pillar arrays stretched [Figure 6(c)] so that the micro-objects escaped under the external vibrate, as shown in Figure 6(d). Moreover, the as-prepared micromechanical hand-like arrays exhibited excellent reproducibility for particle manipulation applications. The particle trapping and releasing process by the same sample could be repeated over 10 cycles.

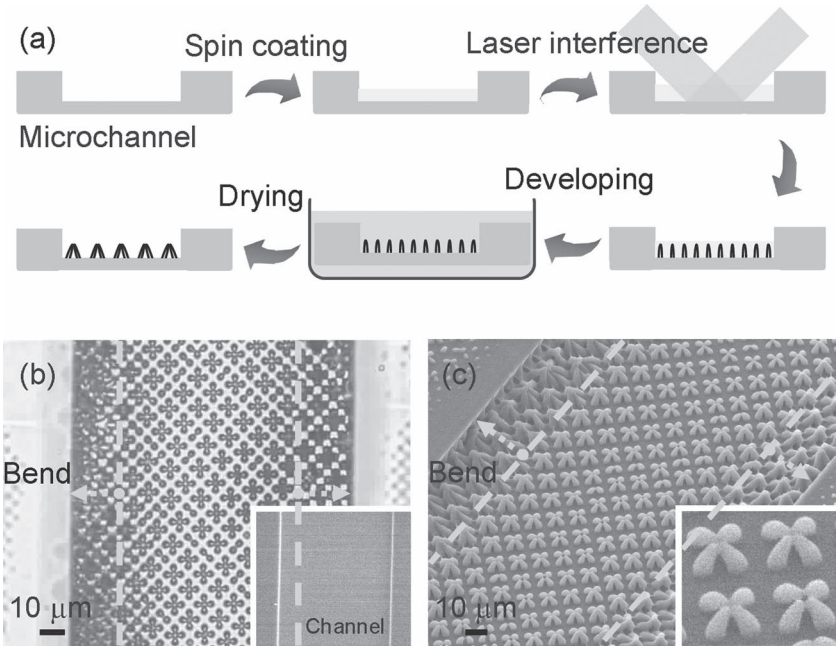

Figure 8. The application of integrating regular 4-pillar-cell arrays into microfluidic devices. (a) The schematic image of the fabrication process. (b) The optical microscopic image of the microstructured microchannel. The inset is the flat microchannel. (c) 45° tilted-view SEM image of microchannel with integrated 4-cell arrays. The inset is its magnified SEM image of 4-cell arrays.

2.5. Integrating Large-Area Assembled Microstructures into Microfluidic Devices

The development of on-chip methods to manipulate microparticles or cells is receiving increasing attention.[19a–b] Here, we not only demonstrated the fabrication of assembled microstructures on flat surface, but also showed the integration of large-area controllable micropatterns into irregular surfaces, for example, microfluidic channel. The combined top-down/bottom-up technique of fabricating regular 3D controllable microarchitectures is compatible with conventional microfabrication methods. By using ultraviolet photolithography to realize the 100 μm-width and 20 μm-depth microchannel, large-area regular microstructures could be integrated into the microchannel by laser interference lithography and capillary force-induced assembly. As shown in **Figure 8**(a), firstly, the photoresist of NOA 61 was spin-coated at 400 rpm/s for 5 μm thicknesses. Then, the sample was irradiated by 355 nm-laser to produce pillar arrays. After developing and drying, the microchannel with integrated microstructures was obtained. Shown in Figure 8(b) is the top-view optical microscopic image of the microstructured channel. In comparison, the inset is the top-view SEM image of the channel without microstructures. Shown in Figure 8(c) is the 45° tilted SEM image of a microchannel with regular 4-cell arrays. The channel was fully filled with the assembled microstructures. It is also worthy to mention that the pillars on both sides of the channel seem to preferentially bend towards the wall of the channel, as shown in the arrow region of Figure 8(b,c). This assembled phenomenon was attributed to the new evaporation-induced capillary force between the pillars and the walls.

3. Conclusion

We have demonstrated a simple strategy to rapidly realize regular controllable microstructures with large-area. A series of capillary force-induced novel microstructures from 2-cell to 12-cell, "S" shape and chain-shape were obtained by controlling the height, shape, width, and arrangement of the pillar arrays prepared by laser interference lithography. This combined top-down/bottom up method is very simple, rapid and cost-effective. Moreover, the application of the assembled microstructures on selectively trapping/releasing microparticles and integrated microfluidic channels were demonstrated. The underlying physical mechanism of reversible particles micromanipulation was investigated as the combined action of the capillary force, the van der Waals force, and the swelling force. This novel technique to manipulate micro-objects by controllable microstructures will show broader applications[20] in engineering, microfluidic and biology.[21]

4. Experimental Section

Materials and Equipment: The commercial photoresisit NOA 61 with excellent elastic property (elasticity modulus ~150 000 psi) was purchased from Norland company. A frequency-tripled, Q-switched, single-mode Nd:YAG laser with about 10 ns pulse width and 355 nm wavelength was purchased from Spectra-physics Company.

The Preparation of the Assembled Microstructures: A glass slide was cleaned with acetone and absolute ethanol, and then the photoresist NOA 61 diluted with acetone (1:1 by volume), was spin-coated at different rotation speeds for difference thicknesses, for example, 500 rpm for 3 μm, 1000 rpm for 1.5 μm, and 1500 rpm for 1 μm. The laser with 355 nm-wavelength and 7 ns pulse width was split into three/four beams and incident into the sample. The

small NANO MICRO

energy of every beam could be precisely controlled by the optical attenuators. The beam diameter is around 1 cm. The photoresist was exposed at 355 nm wavelength laser with different exposure times to control the exposure dosage. Then, the sample was developed in acetone for 1 min to remove the unpolymerized resin and the regular pillar arrays were left. During the solvent evaporation process, various complex 3D microstructures were assembled by controlling the height, shape, width, and arrangement of the pillar arrays.

The Manipulation of Microspheres: The polystyrene sphere was synthesized in aqueous alcohol system. The sodium laurylsulfate and potassium persulfate are used as emulsifier and initiator, respectively. The diameter of the microsphere could be controlled by different aqueous media, e.g., methanol, ethanol, *n*-propyl, as described in previous articles.[22] Then, the microspheres were put into the pillar arrays in solvent. After solvent evaporation, they were trapped by adjacent pillars due to the capillary force.

The Fabrication of Microfluidic Channels: Firstly, a microfluidic channel was fabricated by conventional ultraviolet photolithography. The negative photoresist (SU8 2075, MicroChem) was diluted with cyclopentanone (2:1 by volume) and spin-coated on a cover glass at 500 rpm/s for 20 s. Then, the sample was prebaked at 95 °C for 1 h. After UV exposure on the photomask with the microchannel pattern, it was further postbaked at 95 °C for 10 min to induce the cross-linking process. The pattern was developed for 30 mins and rinsed by acetone. Finally, a microchannel with a 20 μm-height and 100 μm-width was obtained.

Sample Characterization: The morphologies of various assembled microstructures were characterized by a field emission scanning electron microscope (SEM, JSM-7500F, JEOL, Japan). The samples were sputtered with a thin layer of Pt for better SEM imaging. The optical photographs of the samples were taken by OLYMPUS BX51.

Supporting Information

Supporting Information is available from the Wiley Online Library or from the author.

Acknowledgements

This work was supported by NSFC (Grant Nos. 90923037, 60677016, 60525412 and 60877019), NECT (Grant No. 070354) and Jilin Provincial Science and Technology Foundation (Grant No. 20070109).

[1] a) S. Fiedler, S. G. Shirley, T. Schnelle, G. Fuhr, *Anal. Chem.* **1998**, *70*, 1909; b) M. Urdaneta, E. Smela, *Lab Chip* **2008**, *8*, 550.

[2] a) A. Ashkin, J. M. Dziedzic, J. E. Bjorkholm, S. Chu, *Opt. Lett.* **1986**, *11*, 288; b) H. B. Sun, K. Takada, S. Kawata, *Appl. Phys. Lett.* **2001**, *79*, 3173.

[3] a) T. G. Leong, C. L. Randall, B. R. Benson, A. M. Zarafshar, D. H. Gracias, *Lab Chip* **2008**, *8*, 1621; b) T. G. Leong, C. L. Randall, B. R. Benson, N. Bassik, G. M. Stern, D. H. Gracias, *Proc. Natl. Acad. Sci. USA* **2009**, *106*, 703; c) N. Bassik, A. Brafman, A. M. Zarafshar, M. Jamal, D. Luvsanjav, F. M. Selaru, D. H. Gracias, *J. Am. Chem. Soc.* **2010**, *132*, 16314; d) A. Azam, K. E. Laflin, M. Jamal, R. Fernandes, D. H. Gracias, *Biomed. Microdevices* **2011**, *13*, 51.

[4] a) B. Pokroy, S. H. Kang, L. Mahadevan, J. Aizenberg, *Science* **2009**, *323*, 237; b) M. Matsunaga, M. Aizenberg, J. Aizenberg, *J. Am. Chem. Soc.* **2011**, *133*, 5545; c) P. Kim, L. D. Zarzar, X. Zhao, A. Sidorenko, J. Aizenberg, *Soft Matter* **2010**, *6*, 750.

[5] a) S. Park, O. Yavuzcetin, B. Kim, M. T. Tuominen, T. P. Russell, *Small* **2009**, *9*, 1064; b) W. K. Choi, T. H. Liew, H. G. Chew, F. Zheng, C. V. Thompson, Y. Wang, M. H. Hong, X. D. Wang, L. Li, J. Yun, *Small* **2008**, *3*, 330; c) W. K. Choi, T. H. Liew, M. K. Dawood, H. I. Smith, C. V. Thompson, M. H. Hong, *Nano Lett.* **2008**, *8*, 3799; d) J. Y. Cheng, C. A. Ross, H. I. Smith, E. L. Thomas, *Adv. Mater.* **2006**, *18*, 2505.

[6] a) D. Wu, S. Z. Wu, L. G. Liu, Q. D. Chen, R. Wang, J. F. Song, H. H. Fang, H. B. Sun, *Appl. Phys. Lett.* **2010**, *97*, 031109; b) D. Wu, J. N. Wang, S. Z. Wu, Q. D. Chen, S. Zhao, H. Zhang, H. B. Sun, L. Jiang, *Adv. Funct. Mater.* **2011**, *21*, 2927; c) D. Wu, Q. D. Chen, L. G. Niu, J. N. Wang, R. Wang, H. Xia, H. B. Sun, *Lab Chip* **2009**, *9*, 2391.

[7] a) Z. R. Tian, J. Liu, J. A. Voigt, B. Mchenzie, H. Xu, *Angew. Chem. Int. Ed.* **2003**, *42*, 413; b) X. Gao, X. Li, W. Yu, *J. Phys. Chem. B* **2005**, *109*, 1155.

[8] J. W. P. Hsu, Z. R. Tian, N. C. Simmons, C. M. Matzke, J. A. Voigt, J. Liu, *Nano Lett.* **2005**, *5*, 83.

[9] Y. Xia, Y. Yin, Y. Lu, J. Mclellan, *Adv. Funct. Mater.* **2003**, *13*, 907.

[10] M. D. Volder, S. H. Tawfick, S. J. Park, D. Copic, Z. Zhao, W. Lu, A. J. Hart, *Adv. Mater.* **2010**, *22*, 4384.

[11] a) H. Duan, K. K. Berggren, *Nano Lett.* **2010**, *10*, 3710; b) H. Duan, J. K. W. Yang, K. K. Berggren, *Small* **2011**, *18*, 2661.

[12] a) S. H. Kang, B. Pokroy, L. Mahadevan, J. Aizenberg, *ACS Nano* **2010**, *4*, 6323; b) M. Matsunaga, M. Aizenberg, J. Aizenberg, *J. Am. Chem. Soc.* **2011**, 10.1021/ja200241j.

[13] a) J. H. Jang, C. K. Ullal, T. Gorishnyy, V. V. Tsukruk, E. L. Thomas, *Nano Lett.* **2010**, *6*, 740; b) J. H. Jang, C. K. Ullal, S. E. Kooi, C. Y. Koh, E. L. Thomas, *Nano Lett.* **2007**, *7*, 647; c) Y. Wei, W. Wu, R. Guo, D. Yuan, S. Das, Z. L. Wang, *Nano Lett.* **2010**, *10*, 3414; d) A. M. Prenen, J. C. A. H. Werf, C. W. M. Bastiaansen, D. J. Broer, *Adv. Mater.* **2009**, *21*, 1751; e) D. Xia, D. Li, Y. Luo, S. R. J. Brueck, *Adv. Mater.* **2006**, *18*, 930; f) D. Wu, Q. D. Chen, H. Xia, J. Jiao, B. B. Xu, X. F. Lin, Y. Xu, H. B. Sun, *Soft Matter* **2010**, *6*, 263; g) D. Wu, S. Z. Wu, Q. D. Chen, Y. L. Zhang, J. Yao, X. Yao, L. G. Niu, J. N. Wang, L. Jiang, H. B. Sun, *Adv. Mater.* **2011**, *23*, 545; h) J. Y. Cheng, C. A. Ross, H. I. Smith, E. L. Thomas, *Adv. Mater.* **2006**, *18*, 2505.

[14] a) D. Wu, Q. D. Chen, B. B. Xu, J. Jiao, Y. Xu, H. Xia, H. B. Sun, *Appl. Phys. Lett.* **2009**, *95*, 091902; b) J. N. Israelachvili, *Intermolecular and Surface Forces*, 2nd ed., Academic, London **1992**.

[15] S. Z. Wu, D. Wu, J. Yao, Q. D. Chen, J. N. Wang, L. G. Niu, H. H. Fang, H. B. Sun, *Langmuir* **2010**, *26*, 12012.

[16] H. B. Sun, A. Nakamura, S. Shoji, X. M. Duan, S. Kawata, *Adv. Mater.* **2003**, *15*, 2011.

[17] S. Jung, C. Livermore, *Nano Lett.* **2005**, *5*, 2188.

[18] a) Y. Tian, Y. L. Zhang, H. Xia, L. Guo, J. F. Ku, Y. He, R. Zhang, B. Z. Xu, Q. D. Chen, H. B. Sun, *Phys. Chem. Chem. Phys.* **2011**, *13*, 4835; b) K. Takada, D. Wu, Q. D. Chen, S. Shoji, H. Xia, S. Kawata, H. B. Sun, *Opt. Lett.* **2009**, *34*, 566.

[19] a) S. C. McGreehim, T. F. Krauss, K. Dholakia, *Lab Chip* **2006**, *6*, 1122; b) S. Kuhn, P. Measor, E. J. Lunt, B. S. Phillips, D. W. Deamer, A. R. Hawkins, H. Schmidt, *Lab Chip* **2009**, *9*, 2212.

[20] a) B. Su, S. Wang, J. Ma, Y. Song, L. Jiang, *Adv. Funct. Mater.* **2011**, *21*, 3297; b) Y. J. Zhao, H. C. Shum, H. S. Chen, L. L. A. Adams, Z. Z. Gu, D. A. Weitz, *J. Am. Chem. Soc.* **2011**, *133*, 8790.

[21] a) S. M. Block, D. F. Blair, H. C. Berg, *Nature* **1989**, *338*, 514; b) M. P. MacDonald, L. Paterson, K. Volke-Sepulveda, J. Arlt, W. Sibbett, K. Dholakia, *Science* **2002**, *296*, 1101

[22] J. H. Zhang, Z. Chen, Z. L. Wang, W. Y. Zhang, N. B. Ming, *Mater. Lett.* **2003**, *57*, 4466.

Received: July 16, 2012
Published online: November 12, 2012